

APPLIED RESEARCH

Solving Ambiguity in Target Detection for BPSK-Based MIMO FMCW Radar System

JUNHO KIM¹, (Graduate Student Member, IEEE),
YOUNG-JUN YOON², (Associate Member, IEEE), AND
SEONGWOOK LEE¹, (Member, IEEE)

¹School of Electrical and Electronics Engineering, College of ICT Engineering, Chung-Ang University, Dongjak, Seoul 06974, Republic of Korea

²Department of Electrical and Computer Engineering, College of Engineering, Seoul National University (SNU), Gwanak, Seoul 08826, Republic of Korea

Corresponding author: Seongwook Lee (seongwooklee@cau.ac.kr)

This work was supported by the Institute of Information and Communications Technology Planning and Evaluation (IITP) Grant funded by the Korea Government [Ministry of Science and ICT (MSIT)] under Grant 2021-0-00237.

ABSTRACT In a binary phase shift keying (BPSK)-based multiple-input and multiple-output (MIMO) frequency-modulated continuous wave (FMCW) radar system, real and ghost targets are detected simultaneously, causing ambiguity in target detection. In this paper, we define the targets that are inevitably generated by the BPSK modulation as ghost targets and propose a method for suppressing them. The proposed ghost target suppression method consists of two main steps. First, at the receiving end, a received signal is demodulated using a specific code orthogonal to binary codes used to modulate transmitted signals. Due to the Doppler shift caused by the spectrum of the code used at the receiving end, only ghost targets remain in the demodulated received signal. Then, by subtracting the demodulated signal including the ghost targets from the initially received signal, only the information of the actual targets can be restored. We verify the performance of the proposed method through simulations and actual signal measurements. In addition, the target estimation performance of the proposed method is compared with that of the time-division multiplexing MIMO FMCW radar system.

INDEX TERMS Binary phase shift keying, frequency-modulated continuous wave, ghost target, multiple-input and multiple-output.


I. INTRODUCTION

To detect targets with high resolution in the automotive radar system, high range and angular resolution are required. In general, to obtain high range resolution, a frequency-modulated continuous wave (FMCW) [1] using a wide bandwidth is used [2], which has a high pulse compression ratio. In addition, an array antenna composed of multiple antenna elements is widely used to achieve high angular resolution [3]. Recently, a multiple-input and multiple-output (MIMO) antenna system capable of generating a large number of receiving channels in a limited space has been adopted [4].

To estimate the distance, velocity, and angle information of a target using the MIMO FMCW radar system, signals

transmitted from each antenna element must be distinguished at the receiving end [5]. Therefore, the antenna system adopts a time-division multiplexing (TDM) [6], [7], a frequency-division multiplexing [8], [9], or a code-division multiplexing [10], [11] to transmit FMCW radar signals. Currently, the TDM-based MIMO scheme is most commonly used, but it has a disadvantage in that the maximum detectable velocity is reduced in proportion to the number of transmit antenna elements [12]. In addition, the time delay between the waveforms transmitted from different antenna elements greatly degrades the angle estimation accuracy [13].

To solve these issues of the TDM-based MIMO FMCW radar system, a binary phase shift keying (BPSK)-based MIMO FMCW radar system [14] can be considered. In the BPSK-based MIMO FMCW radar system, signals to which the binary phase modulation is applied are transmitted. A decrease in the maximum detectable velocity can be

The associate editor coordinating the review of this manuscript and approving it for publication was Cheng Hu .

avoided through the binary phase modulation, but ghost targets are detected along the Doppler axis [15], [16]. To distinguish between real and ghost targets in this system, the intensity of the received signal can be used [15]. In addition, the authors in [17] used the Chinese remainder theorem (CRT) to resolve ambiguities in target detection. However, the method proposed in [15] cannot be used in a complex road environment in which multiple targets exist at the same time. Moreover, target detection results in multiple consecutive frames are required to resolve the Doppler ambiguity in the CRT-based method [17], not resolving in a single frame.

In this paper, we propose a method for identifying ghost targets at the receiving end by decoding the received signal with the proposed code and extracting only actual targets by removing the identified ghost targets from the range-Doppler map. In summary, the major contributions of our work can be summarized as follows :

- Through the proposed decoding method, ghost targets generated by the binary phase code can be extracted clearly.
- Unlike the methods proposed in [15] and [17], the desired signal corresponding to the actual target can be obtained simply by suppressing the ghost targets with the proposed method.
- Compared with target detection results in the TDM-based MIMO FMCW radar system, the decrease of the maximum detectable velocity could be overcome in the BPSK-based MIMO FMCW radar system with the proposed method.

The remainder of this paper is organized as follows. In Section II, we describe the basic principle of the BPSK-based MIMO FMCW radar system. Then, in Section III, a method for removing ghost targets in the BPSK-based MIMO FMCW radar system is proposed. In addition, the performance of the proposed method is compared with that of the TDM-based MIMO FMCW radar system in this section. In Section IV, we verify the performance of the proposed method through actual signal measurements. Finally, we conclude this paper in Section V.

II. SYSTEM MODEL

A. SIGNAL MODEL IN MIMO FMCW RADAR SYSTEM

For simplicity, we first describe transmitted and received signals in a single-input and single-output FMCW radar system. In the FMCW radar system, a transmitted signal consists of a series of chirps. The p -th ($p = 1, 2, \dots, N_c$) chirp of the transmitted signal in $(p-1)\Delta t \leq t < p\Delta t$ can be expressed as

$$s_p(t) = \alpha_p \exp \left(j \left(2\pi \left(f_c - \frac{2p-1}{2} \Delta f \right) t + \pi \frac{\Delta f}{\Delta t} t^2 + \phi_p \right) \right), \quad (1)$$

where α_p and ϕ_p represent the amplitude and phase offset of the p -th chirp. In addition, f_c , Δf , and Δt indicate the center frequency, bandwidth, and chirp duration of each

chirp, respectively. Then, the transmitted signal of one period including all chirps can be expressed as

$$s(t) = \begin{cases} s_p(t) & \text{for } (p-1)\Delta t \leq t < p\Delta t \\ 0 & \text{for } N_c\Delta t \leq t < \Delta T, \end{cases} \quad (2)$$

where ΔT indicates the transmission period. In addition, the received signal can be expressed as

$$y(t) = \sum_{k=1}^{N_K} \beta_k s(t - \tau_k) + n(t), \quad (3)$$

where β_k is the amplitude of the received signal and τ_k is the time delay caused by the distance (d_k) and velocity (v_k) of the k -th target. In addition, N_K is the number of targets and $n(t)$ is the noise added at the receiving antenna element.

Now, consider a MIMO antenna system in which the number of transmit antenna elements is N_T and the number of receiving antenna elements is N_R . When the signal transmitted by all q ($q = 1, 2, \dots, N_T$) transmit antenna elements is received by the r -th ($r = 1, 2, \dots, N_R$) receiving antenna element, it can be expressed

$$y_r(t) = \sum_{q=1}^{N_T} \left(\sum_{k=1}^{N_K} \beta_k s \left(t - (\tau_k + u_{q,k} + v_{r,k}) \right) \right) + n_r(t), \quad (4)$$

where $n_r(t)$ is the noise added at the r -th receiving antenna element. In (4), $u_{q,k}$ and $v_{r,k}$ denote the time delays due to the spacing (d_T) between the transmit antenna elements and the spacing (d_R) between the receiving antenna elements, respectively. If the angle between the k -th target and the boresight of the antenna is denoted as θ_k , the total time delay caused by the antenna spacing can be expressed as

$$u_{q,k} + v_{r,k} = \frac{2\pi}{\lambda} \left((q-1)d_T + (r-1)d_R \right) \sin \theta_k, \quad (5)$$

where λ is the wavelength corresponding to the center frequency of the FMCW radar signal.

B. BPSK MODULATION FOR MIMO FMCW RADAR

In the BPSK-based MIMO FMCW radar system, the FMCW radar signal transmitted from the q -th antenna element is modulated as

$$x_q(t) = s(t) \exp \left(j\pi c_q(t) \right), \quad (6)$$

where $c_q(t)$ is a code assigned to the q -th antenna element for the BPSK modulation. In general, orthogonal codes are used as $c_q(t)$ to lower the cross-correlation between signals transmitted from different antenna elements. For example, Hadamard code [18] can be used for the BPSK modulation. In this paper, the binary codes are assigned by dividing the total number of chirps by units of $\frac{N_c}{L_c}$, which can be expressed as

$$c_q(t) = \sum_{m=1}^{\frac{N_c}{L_c}} g_q \left(t - (m-1)L_c\Delta t \right), \quad (7)$$

where $g_q(t)$ exists between $0 \leq t < L_c \Delta t$ and has a value of 1 or -1 every Δt . Here, we set N_c to be a multiple of L_c so that $\frac{N_c}{L_c}$ becomes an integer. In addition, $g_q(t)$ satisfies the property of being orthogonal to each other, which can be expressed as

$$\frac{1}{L_c \Delta t} \int_0^{L_c \Delta t} g_i(t) g_j(t) dt = \begin{cases} 0 & \text{for } i \neq j \\ 1 & \text{for } i = j. \end{cases} \quad (8)$$

In the FMCW radar system, the received signal is down-converted to a baseband signal by passing through a frequency mixer and a low-pass filter. In general, the time delays, τ_k , $u_{q,k}$, and $v_{r,k}$, are very small compared to Δt , which means $c_q(t - (\tau_k + u_{q,k} + v_{r,k})) \cong c_q(t)$. Thus, the signal transmitted from the q -th transmit antenna element is sampled by the analog-to-digital converter at the r -th receiving antenna element, and it can be expressed as a two-dimensional signal as follows:

$$z_{q,r}[n, p] = \sum_{k=1}^{N_k} \gamma_k e^{j\pi c_q(nT_s + (p-1)\Delta t)} \times \exp \left(j2\pi \left(\frac{2d_k \Delta f}{c \Delta t} nT_s + \frac{2v_k f_c \Delta t}{c} p + u_{q,k} + v_{r,k} + \frac{2d_k f_c}{c} \right) \right), \quad (9)$$

where n ($n = 1, 2, \dots, N_s$) is the index of the time samples at each chirp and T_s is the sampling interval. In addition, γ_k denotes the amplitude of the k -th baseband signal. In the MIMO antenna system, the signal received by the r -th antenna element is the sum of signals transmitted by all transmit antenna elements, which can be expressed as follows:

$$z_r[n, p] = \sum_{q=1}^{N_T} z_{q,r}[n, p]. \quad (10)$$

For example, consider a BPSK-based MIMO radar system with 3 transmit antenna elements, and assume that each antenna element uses orthogonal Hadamard codes as follows: $g_1(t) = [0, 0, 0, 0]$, $g_2(t) = [1, 0, 1, 0]$, $g_3(t) = [1, 1, 0, 0]$, which is shown in Fig. 1. In this example, the system parameter values related to the FMCW radar were set to values widely used in commercial automotive radar systems [19], and they are given in Table 1. As given in the table, we assumed a 3 by 16 MIMO antenna system with a spacing of 0.45λ between all antenna elements, and the antenna layout of the MIMO radar system in the simulation environment is shown in Fig. 2. The information of targets is also given in Table 2.

The signals transmitted from each transmit antenna elements are shifted along the Doppler axis by assigned binary phase codes [15], and Fig. 3 shows the Doppler shift according to the spectrum of the code assigned by each transmit antenna element. In the case of Fig. 3 (a), the transmitted signal coded with $g_1(t)$ does not affect the phase. Therefore, the Doppler shift does not appear and the detection result of the

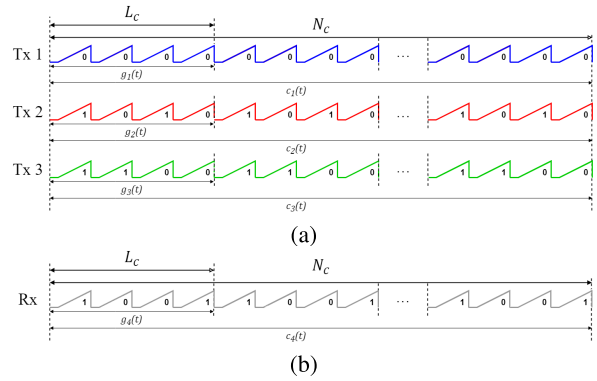


FIGURE 1. Orthogonal codes used (a) for the transmitted signals and (b) at the receiving end in the proposed BPSK-based radar system.

TABLE 1. System parameters and their values used in the simulation.

System parameters	Values
Center frequency, f_c	77 GHz
Wavelength, λ	3.8961 mm
Bandwidth, Δf	2 GHz
Chirp duration, Δt	100 μ s
The number of chirps, N_c	256
The number of time samples, N_s	1024
Sampling frequency, f_s	10.24 MHz
The number of transmit antenna elements, N_T	3
The number of receiving antenna elements, N_R	16
Antenna spacing between antenna elements, d_T and d_R	1.7532 mm

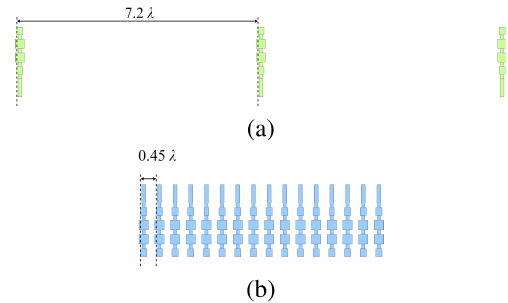


FIGURE 2. Schematic diagram for the (a) transmit and (b) receiving antenna elements of the MIMO radar system.

TABLE 2. Target information in the simulation.

Target information	Target 1	Target 2	Target 3
Distance, d_k (m)	5	10	15
Velocity, v_k (m/s)	0	2	5
Angle, θ_k (deg.)	0	30	45

actual target is maintained. However, in Figs. 3 (b) and (c), the transmitted signals are shifted along the Doppler axis by the binary phase codes and show different Doppler shifts depending on the spectrum of the code.

To understand the effect of the signal multiplied by the code at each transmit antenna, we decomposed the signal received from the r -th receiving antenna element, as shown in Figs. 4 (a), (b), and (c). In reality, three transmitted signals are combined and received as shown in Fig. 4 (d). As described in Fig. 3, the positions of the detected targets move along the Doppler axis. In this study, we define targets other than actual target as ghost targets. To extract actual targets only, an efficient method capable of suppressing ghost targets occurring at the receiving end is required.

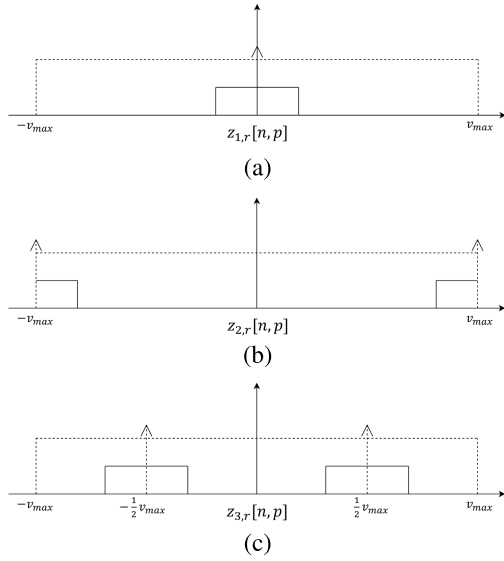


FIGURE 3. Doppler shifts of range-Doppler maps in the BPSK modulation: (a) Tx 1, (b) Tx 2, and (c) Tx 3.

III. PROPOSED GHOST TARGET SUPPRESSION METHOD

A. IDENTIFICATION OF GHOST TARGETS

First, we propose a method of extracting only ghost targets from the receiving end. Unlike previous studies, we use $N_T + 1$ codes for the BPSK modulation, which means the number of $c_q(t)$ becomes $N_T + 1$, not N_T . The transmit end uses the 1st to N_T -th codes, and the last $(N_T + 1)$ -th code is used by the receiving end. If $z_r[n, p]$ is multiplied with the proposed code $e^{j c_{N_T+1}(t)}$, the decoded received signal can be expressed as

$$\tilde{z}_r[n, p] = z_r[n, p] \times e^{j c_{N_T+1}(t)}. \quad (11)$$

When the received signal is decoded by the proposed method, the Doppler shift occurs due to the code multiplied at the receiving end, as shown in Fig. 5. Therefore, the actual target information disappears and only the Doppler shifted signals remain. In other words, the signal components corresponding to the actual targets were removed from the received signal and only ghost targets can be extracted by decoding the received signal with the proposed code. For example, the result of decoding the received signal with the proposed method for the target detection result in Fig. 4 (d) is shown in Fig. 6. At the receiving end, a code $c_4(t)$, which is orthogonal to $c_1(t)$, $c_2(t)$, and $c_3(t)$, is used as shown in Fig. 1 (b). As shown in the figure, when the code $c_4(t)$ is multiplied by the received signal, only the information of the actual targets disappears from the range-Doppler map.

B. EXTRACTION OF ACTUAL TARGETS

Using the proposed decoding method in III-A, only ghost targets can be identified in the range-Doppler map. Then, to extract only real targets from the range-Doppler map where the ghost and real targets exist at the same time, a method of subtracting the two signals is proposed. In other words, by using the signals of (10) and (11), only desired target

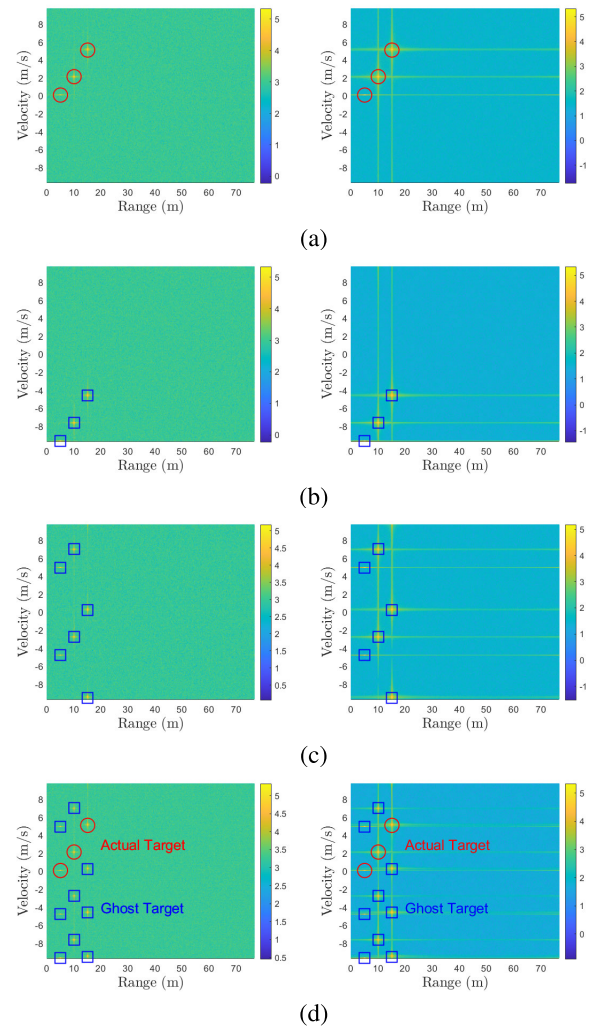


FIGURE 4. Range-Doppler maps in the BPSK-based MIMO FMCW radar system with 0 dB and 30 dB SNR value: when the signal transmitted from the (a) Tx 1, (b) Tx 2, (c) Tx 3, and (d) all transmit antenna elements.

information can be extracted, which can be expressed as

$$d_r[n, p] = |z_r[n, p]| - \delta |\tilde{z}_r[n, p]|, \quad (12)$$

where δ is a constant for correcting the signal strength between two signals, $z_r[n, p]$ and $\tilde{z}_r[n, p]$. When the maximum value of the peaks shown in $z_r[n, p]$ including the real and ghost targets is denoted as $z_{r, \max}$ and the minimum value of the peaks shown in $\tilde{z}_r[n, p]$ from which only ghost targets are extracted by multiplying the code is denoted as $\tilde{z}_{r, \min}$, δ is set to $z_{r, \max} / \tilde{z}_{r, \min}$. Finally, as shown in Fig. 7, all ghost targets have been removed through the proposed method and only information on real targets remains in the range-Doppler map. As shown in the simulation results, the proposed method was well applied at various signal-to-noise ratio (SNR) values.

C. PERFORMANCE COMPARISON WITH TDM-BASED MIMO FMCW RADAR SYSTEM

In this section, we compare the target detection performance of the proposed method with that of the TDM-based MIMO

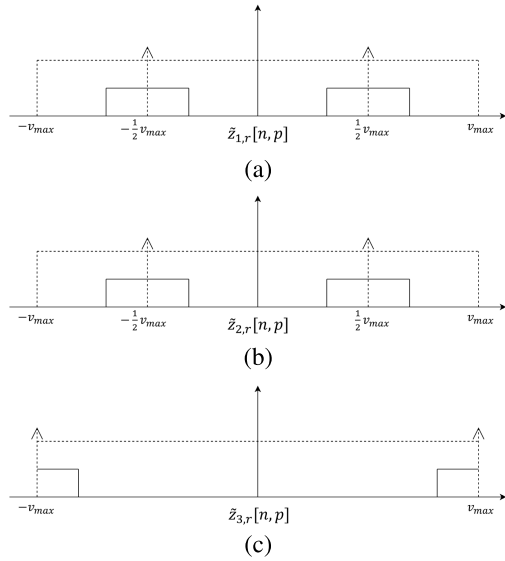


FIGURE 5. Doppler shifts of range-Doppler maps with the proposed code in the BPSK modulation: (a) Tx 1, (b) Tx 2, and (c) Tx 3.

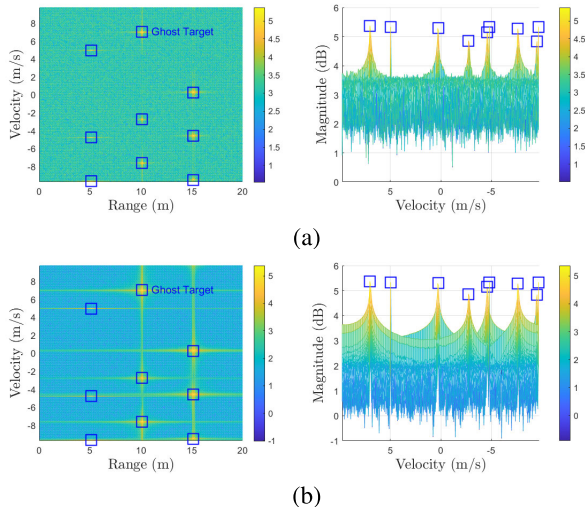


FIGURE 6. Range-Doppler maps after multiplying the code at the receiving end: when the SNR value is (a) 0 dB and (b) 30 dB.

FMCW radar system. Both BPSK-based and the TDM-based MIMO FMCW radar systems share the same system parameter values given in Table 1. The signals transmitted in both methods are shown in Fig. 8. The main differences between the two transmission methods are summarized as follows. In the BPSK-based MIMO FMCW radar, N_c chirps are transmitted from all N_T antenna elements at the same time. On the other hand, in the TDM-based MIMO FMCW radar, a total of N_c chirps are transmitted alternately on a total of N_T antenna elements, as shown in the figure.

Fig. 9 shows the range-Doppler maps in the TDM-based MIMO FMCW radar system and the BPSK-based MIMO FMCW radar system with the proposed decoding method. As shown in Figs. 9 (a) and (b), the velocities of the Targets 1 and 2 are accurately estimated in both radar systems. However, the velocity of target 3 was estimated to be -1.494 m/s instead of 5 m/s in the TDM-based MIMO

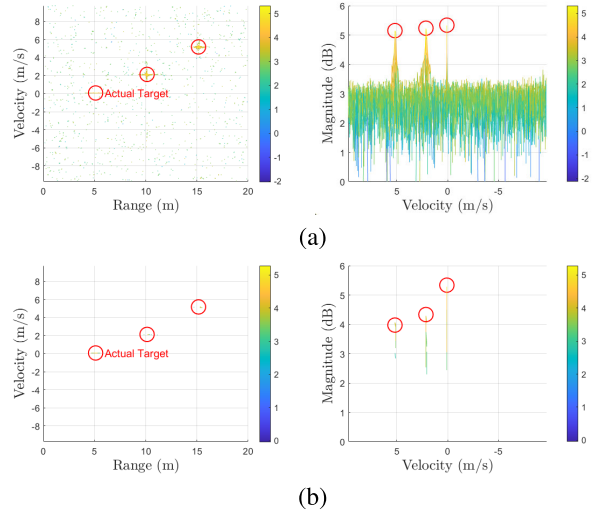


FIGURE 7. Range-Doppler maps after removing extracted ghost targets: when the SNR value is (a) 0 dB and (b) 30 dB.

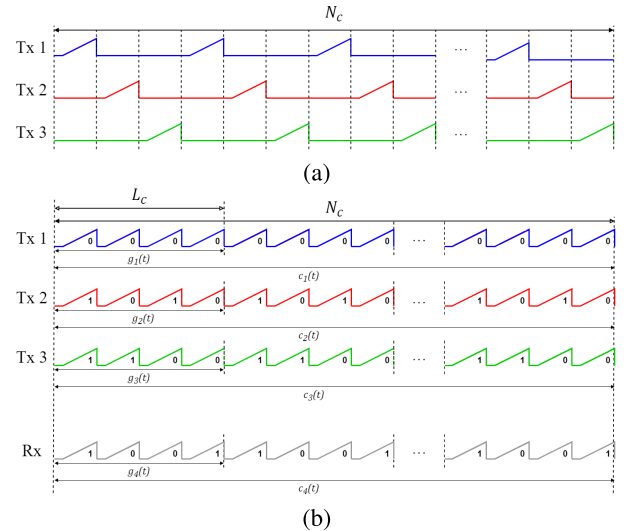


FIGURE 8. Signals used in the (a) TDM-based and (b) BPSK-based MIMO FMCW radar systems.

FMCW radar system. In the TDM-based MIMO FMCW radar system, the chirp duration increases in proportion to the number of transmit antenna elements. Therefore, the maximum detectable velocity is decreased from $v_{\max} = \frac{\lambda}{4\Delta t}$ to $v_{\max, \text{TDM}} = \frac{\lambda}{4N_T \Delta t}$ [12]. Thus, the maximum detectable velocity in the simulation decreases to 3.247 m/s proportional to N_T . If the velocity without ambiguity is denoted as v_{unamb} , the ambiguous velocity can be expressed as $v_{\text{amb}} = v_{\text{unamb}} + l \times v_{\max, \text{TDM}}$, where l is the integer. Thus, the velocity of Target 3 moving at 5 m/s was estimated to be -1.494 m/s (i.e., $-1.494 = 5 - 2 \times 3.247$). However, when the target was detected by the proposed decoding method in the BPSK-based MIMO FMCW radar system, distance and velocity information for three targets was accurately extracted in the range-Doppler map, as shown in Fig. 9 (b). In summary, compared to the TDM modulation scheme, the ambiguity in the target velocity estimation disappears.

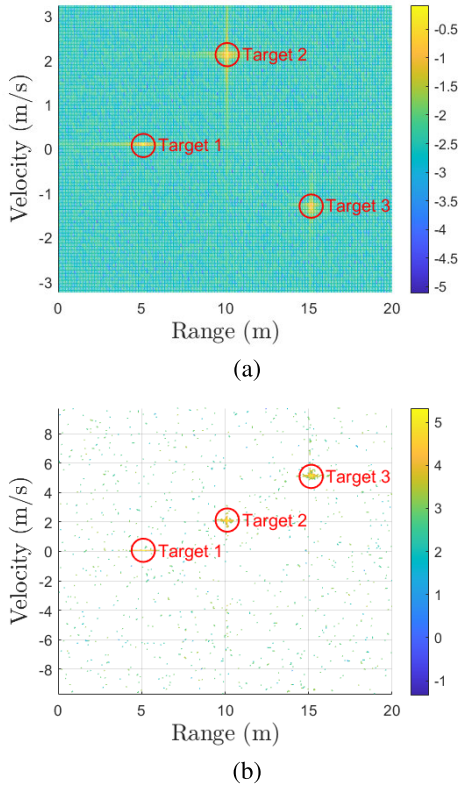


FIGURE 9. Range-Doppler maps (a) in the TDM-based MIMO FMCW radar system and (b) when applying the proposed decoding method in the BPSK-based MIMO FMCW radar system.

TABLE 3. Specifications of the MIMO FMCW radar system.

System parameters	Values
Center frequency, f_c	77 GHz
Wavelength, λ	3.8961 mm
Bandwidth, Δf	2.01 GHz
Chirp duration, Δt	500 μ s
Frame time, t_f	128 ms
The number of chirps, N_c	256
The number of time samples, N_s	256
Sampling frequency, f_s	10 MHz
The number of transmit antenna elements, N_T	3
The number of receiving antenna elements, N_R	16
Antenna spacing between antenna elements, d_T and d_R	1.9481 mm

TABLE 4. Target information in the measurement.

Target information	Stationary target	Moving target
Distance, d_k (m)	5	5
Velocity, v_k (m/s)	0	0.72
Angle, θ_k (deg.)	0	-30

IV. PERFORMANCE EVALUATION THROUGH ACTUAL MEASUREMENTS

A. MEASUREMENT ENVIRONMENT

In this section, the performance of the proposed method is verified using signals obtained by an automotive radar sensor. In the experiment, we used the MMWCAS-RF-EVM manufactured by Texas Instruments, which is a cascade of 4 AWR2243 MIMO FMCW radar chips [20]. This radar system provides a function to apply the BPSK modulation to the transmitted signals and also support the TDM

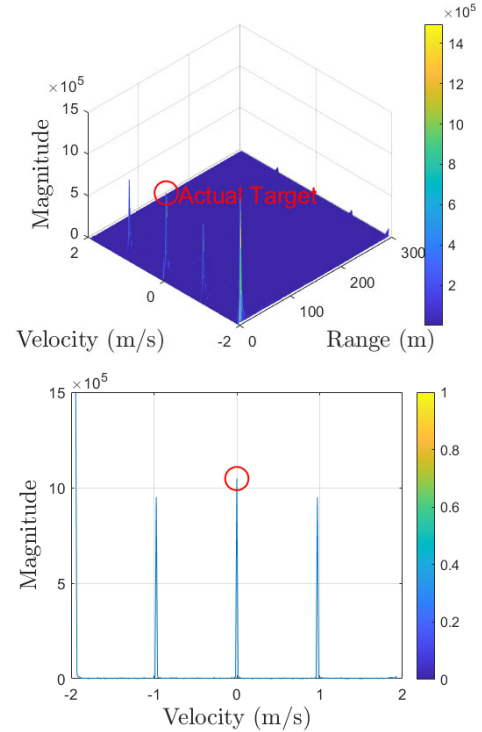


FIGURE 10. Target detection results on the range-Doppler maps and the Doppler axes for the stationary target in the BPSK-based MIMO FMCW radar system before applying the proposed decoding method.

transmission scheme. The radar sensor uses 77 GHz and 2.01 GHz as the center frequency and the bandwidth, respectively. In addition, 256 chirps were used in both TDM and BPSK modulations, and 256 time samples were obtained at each chirp. Also, the chirp duration was set to 500 μ s, so the total frame time was 128 ms (i.e., 500 μ s \times 256 = 128 ms). We set the same frame time for both TDM and BPSK modulations, so that the target detection period is the same in both cases. Moreover, the number of transmit antenna elements and the number of receiving antenna elements used in our measurements were 3 and 16, respectively. The specifications of the radar sensor we used are summarized in Table 3. This radar was used to acquire radar sensor data for stationary and moving targets, and the information of the targets are given in Table 4. As a target, a trihedral corner reflector made of iron with a side length of 20 cm was used.

B. PERFORMANCE COMPARISON WITH TDM-BASED MIMO FMCW RADAR SYSTEM

Fig. 10 shows an initial range-Doppler map for the stationary target in the BPSK-based MIMO FMCW radar system. In this case, as in the simulation environment, the codes $c_1(t)$, $c_2(t)$, $c_3(t)$, and $c_4(t)$ in Fig. 1 were used for each transmit antenna element and the receiving end. As shown in the figure, three ghost targets are additionally detected by the codes. Then, the result of suppressing the ghost targets by applying the proposed decoding method is shown in Fig. 11. As shown in the figure, ghost targets are effectively removed even in actual radar systems.

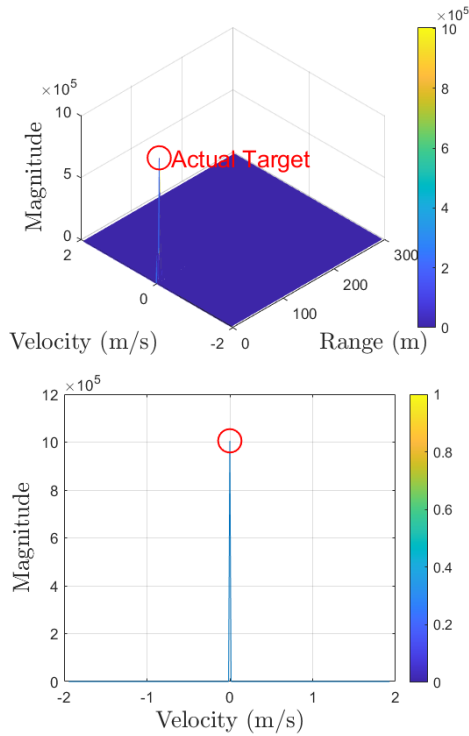


FIGURE 11. Target detection results on the range-Doppler maps and the Doppler axes for the stationary target in the BPSK-based MIMO FMCW radar system after applying the proposed decoding method.

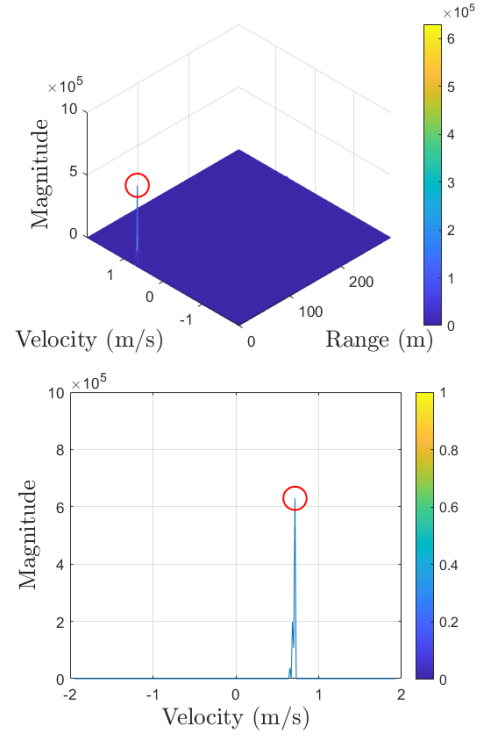


FIGURE 13. Target detection results on the range-Doppler maps and the Doppler axes of the moving target in the BPSK-based MIMO FMCW radar system with the proposed decoding method.

TABLE 5. Time duration required for detecting the target.

Methods	Time duration (s)
TDM modulation	1.456
BPSK modulation	1.333
BPSK modulation with the proposed method	1.992

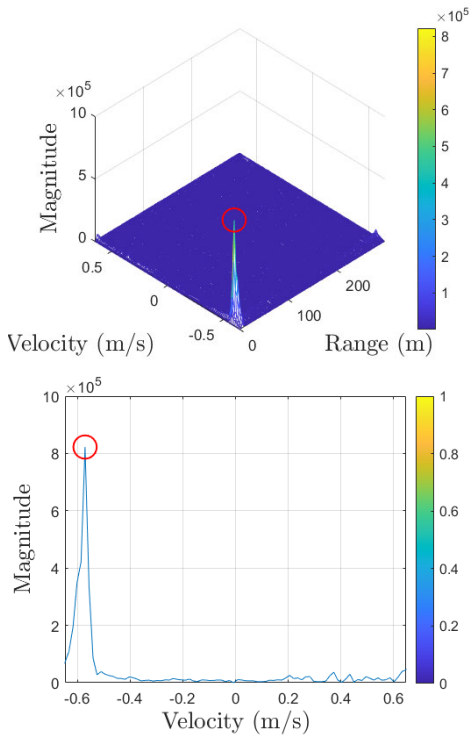


FIGURE 12. Target detection results on the range-Doppler maps and the Doppler axes of the moving target in the TDM-based MIMO FMCW radar system.

In addition, the performance of the proposed method was verified by comparing it with that of the TDM-based MIMO FMCW radar system. Based on the radar system of the

specifications in Table 3, the maximum detectable velocity decreases from 1.9443 m/s to 0.6481 m/s in the TDM modulation. Fig. 12 shows the detection results for the moving target in the TDM-based MIMO FMCW radar system. As given in the Table 4, the velocity of the moving target is 0.72 m/s, which exceeds the maximum detectable velocity of the TDM-based MIMO FMCW radar system. Thus, the velocity of the moving target is detected as a velocity with ambiguity beyond the maximum detectable velocity (i.e., $-0.576 = 0.72 - 2 \times 0.6481$). However, in Fig. 13, when the proposed decoding method is used with the BPSK modulation, the velocity of the moving target was accurately detected as 0.72 m/s.

Moreover, the times required for detecting the target were measured for the TDM modulation, BPSK modulation, and BPSK modulation with the proposed ghost target suppression method, which is shown in Table 5. This time means the duration taken to output the final detection result by applying the constant false alarm rate algorithm to the received signal, and it was computed based on the Intel (R) Core (TM) i5-11600K processor and Samsung DDR4 16G PC4-25600. As shown in the table, the time duration of the BPSK-based MIMO FMCW radar system with the proposed ghost target suppression method is longer than those of conventional TDM and

BSPK modulation schemes. Although the calculation time is increased compared to the TDM-based MIMO FMCW radar system, the proposed method overcomes the reduction in the maximum detectable velocity, so it can be efficiently applied in an environment where vehicles are moving at high velocities.

V. CONCLUSION

In this paper, we proposed a method for identifying ghost targets and suppressing them in the BPSK-based MIMO FMCW radar system. At the receiving end, by using the code orthogonal to the codes used by the transmit antenna elements, only ghost targets was extracted. Then, information about the distance and velocity of the ghost targets was suppressed by subtracting the decoded received signal from the initially received signal. The performance of the proposed method was verified through simulations and actual signal measurements. In the TDM-based MIMO FMCW radar system, target detection is performed in one step, whereas our proposed method requires one more step, ghost target identification, for target detection. However, the decrease of the maximum detectable velocity in the TDM-based MIMO FMCW radar system could be overcome through the proposed method, which is the most important factor determining radar performance.

REFERENCES

- [1] V. Winkler, "Range Doppler detection for automotive FMCW radars," in *Proc. Eur. Microw. Conf.*, Oct. 2007, pp. 166–169.
- [2] Y. Cheng, X. Wang, T. Caelli, X. Li, and B. Moran, "On information resolution of radar systems," *IEEE Trans. Aerosp. Electron. Syst.*, vol. 48, no. 4, pp. 3084–3102, Oct. 2012.
- [3] H. Sun, F. Brigui, and M. Lesturgie, "Analysis and comparison of MIMO radar waveforms," in *Proc. Int. Radar Conf. (RADAR)*, Lille, France, Oct. 2014, pp. 1–6.
- [4] S. Rao. *MIMO Radar*. Texas Instruments, Dallas, TX, USA. [Online]. Available: <https://www.ti.com/lit/an/swra554a/swra554a.pdf>
- [5] J. Li and P. Stoica, *MIMO Radar Signal Processing*. Hoboken, NJ, USA: Wiley, 2009.
- [6] X. Li, X. Wang, Q. Yang, and S. Fu, "Signal processing for TDM MIMO FMCW millimeter-wave radar sensors," *IEEE Access*, vol. 9, pp. 167959–167971, 2021.
- [7] A. Zwanetski and H. Rohling, "Continuous wave MIMO radar based on time division multiplexing," in *Proc. 13th Int. Radar Symp.*, Warsaw, Poland, May 2012, pp. 119–121.
- [8] D. Cohen, D. Cohen, and Y. C. Eldar, "High resolution FDMA MIMO radar," *IEEE Trans. Aerosp. Electron. Syst.*, vol. 56, no. 4, pp. 2806–2822, Aug. 2020.
- [9] A. Zwanetski, M. Kronauge, and H. Rohling, "Waveform design for FMCW MIMO radar based on frequency division," in *Proc. 14th Int. Radar Symp.*, Dresden, Germany, Jun. 2013, pp. 89–94.
- [10] J. J. M. De Wit, W. L. Van Rossum, and A. J. De Jong, "Orthogonal waveforms for FMCW MIMO radar," in *Proc. IEEE Radar Conf.*, Kansas City, MO, USA, May 2011, pp. 686–691.
- [11] S. Hamidi and S. S. Naeini, "CDM based virtual FMCW MIMO radar imaging at 79 GHz," in *Proc. IEEE Can. Conf. Electr. Comput. Eng. (CCECE)*, Sep. 2021, pp. 1–4.
- [12] F. Roos, J. Bechter, N. Appenrodt, J. Dickmann, and C. Waldschmidt, "Enhancement of Doppler unambiguity for chirp-sequence modulated TDM-MIMO radars," in *IEEE MTT-S Int. Microw. Symp. Dig.*, Munich, Germany, Apr. 2018, pp. 1–4.
- [13] C. M. Schmid, R. Feger, C. Pfeffer, and A. Stelzer, "Motion compensation and efficient array design for TDMA FMCW MIMO radar systems," in *Proc. 6th Eur. Conf. Antennas Propag. (EUCAP)*, Prague, Czech Republic, Mar. 2012, pp. 1746–1750.
- [14] S. M. Patole, M. Torlak, D. Wang, and M. Ali, "Automotive radars: A review of signal processing techniques," *IEEE Signal Process. Mag.*, vol. 34, no. 2, pp. 22–35, Mar. 2017.
- [15] Y. L. Sit, G. Li, S. Manchala, H. Afrasiabi, C. Sturm, and U. Lubbert, "BPSK-based MIMO FMCW automotive-radar concept for 3D position measurement," in *Proc. 15th Eur. Radar Conf. (EuRAD)*, Madrid, Spain, Sep. 2018, pp. 289–292.
- [16] J. Jung, S. Lim, S.-C. Kim, and S. Lee, "Solving Doppler-angle ambiguity of BPSK-MIMO FMCW radar system," *IEEE Access*, vol. 9, pp. 120347–120357, 2021.
- [17] H. A. Gonzalez, C. Liu, B. Vogginger, and C. G. Mayr, "Doppler ambiguity resolution for binary-phase-modulated MIMO FMCW radars," in *Proc. Int. Radar Conf. (RADAR)*, Toulon, France, Sep. 2019, pp. 1–6.
- [18] X. Qina, X. Yang, and W. Jiang, "Amplitude-fluctuation separation based on BPM waveform reconstruction in MIMO systems," in *Proc. 3rd Int. Conf. Data Mining, Commun. Inf. Technol.*, Beijing, China, May 2019, pp. 1–8.
- [19] J. Hatch, A. Topak, R. Schnabel, T. Zwick, R. Weigel, and C. Waldschmidt, "Millimeter-wave technology for automotive radar sensors in the 77 GHz frequency band," *IEEE Trans. Microw. Theory Techn.*, vol. 60, no. 3, pp. 845–860, Mar. 2012.
- [20] (2022). *AWR2243 Single-Chip 76- to 81-GHz FMCW Transceiver*. [Online]. Available: <https://www.ti.com/lit/ds/symlink/awr2243.pdf>



JUNHO KIM (Graduate Student Member, IEEE)

received the B.S. degree in electronics and information engineering from Korea Aerospace University (KAU), Goyang, Gyeonggi, Republic of Korea, in February 2022. He is currently pursuing the M.S. degree with Chung-Ang University (CAU), Seoul, Republic of Korea. His research interests include signal processing for automotive radar systems, such as waveform design and modulation schemes, target recognition, and classification with deep learning applications.



YOUNG-JUN YOON (Associate Member, IEEE) received the B.S. degree in electrical and computer engineering from the University of Seoul, Seoul, Republic of Korea, in February 2015. He is currently pursuing the Ph.D. degree with Seoul National University, Seoul. His research interests include the physical layer of communication systems, such as physical layer security and active eavesdropping, communications channel modeling, radar signal processing, and deep learning applications.



SEONGWOOK LEE (Member, IEEE) received the B.S. and Ph.D. degrees in electrical and computer engineering from Seoul National University (SNU), Seoul, Republic of Korea, in February 2013 and August 2018, respectively. From September 2018 to February 2020, he was a Staff Researcher with the Machine Learning Laboratory, AI and SW Research Center, Samsung Advanced Institute of Technology (SAIT), Gyeonggi, Republic of Korea. He was an Assistant Professor with the School of Electronics and Information Engineering, College of Engineering, Korea Aerospace University (KAU), Gyeonggi, from March 2020 to February 2023. Since March 2023, he has been an Assistant Professor with the School of Electrical and Electronics Engineering, College of ICT Engineering, Chung-Ang University (CAU), Seoul. He published more than 90 articles on signal processing for radar systems. His research interests include radar signal processing techniques, such as enhanced target detection and tracking, target recognition and classification, clutter suppression and mutual interference mitigation, and artificial intelligence algorithms for radar systems.